Global analysis of the Higgs candidate with mass $\sim 125\,$GeV

John Ellis[a,b] **and Tevong You**[b,c]

[a] *Theoretical Particle Physics and Cosmology Group, Physics Department,*
 King's College London, London WC2R 2LS, U.K.

[b] *TH Division, Physics Department, CERN,*
 CH-1211 Geneva 23, Switzerland

[c] *High Energy Physics Group, Blackett Laboratory, Imperial College,*
 Prince Consort Road, London SW7 2AZ, U.K.

 E-mail: john.ellis@cern.ch, tevong.you@kcl.ac.uk

ABSTRACT: We analyze the properties of the Higgs candidate with mass $\sim 125\,$GeV discovered by the CMS and ATLAS Collaborations, constraining the possible deviations of its couplings from those of a Standard Model Higgs boson. The CMS, ATLAS and Tevatron data are compatible with Standard Model couplings to massive gauge bosons and fermions, and disfavour several types of composite Higgs models unless their couplings resemble those in the Standard Model. We show that the couplings of the Higgs candidate are consistent with a linear dependence on particle masses, scaled by the electroweak scale $v \sim 246\,$GeV, the power law and the mass scale both having uncertainties $\sim 20\%$.

Contents

1   Introduction and summary

The hint of a possible new particle h with mass $\sim 125\,\mathrm{GeV}$ reported earlier by the LHC experiments ATLAS and CMS [1–14], has now become an indisputable discovery [15–26, 28], which has been supported by new analyses from the Tevatron collider experiments CDF and D0 [29, 30]. There is a general expectation that h may be the long-sought Higgs boson [31–36], but many consistency checks must be made before this identification can be confirmed. For example, it will be necessary to verify that the spin of the h particle is zero [37] — the assignment assumed in searches in the WW^* and ZZ^* channels, which is also consistent with the observation of h decay into $\gamma\gamma$ — and one would like to verify that the couplings of the h to other particles are proportional to their masses. Moreover, even if the h particle passes these tests, other measurements and consistency checks will be needed to see whether it stands alone or is the first representative of a more complicated, possibly composite, electroweak symmetry-breaking sector.

Assuming that the h particle does indeed have spin zero, in this paper we explore the extent to which its couplings are constrained by the available data, studying what limits can already be set on possible deviations from those of a Standard Model Higgs boson ([38–42]; for papers subsequent to the h discovery that are similar in spirit to ours, see, [43–50]). We treat as independent parameters the strengths of the h couplings to massive vector bosons and to different fermion species, including their indirect effects on loop-induced couplings

to photon and gluon pairs and assuming that the latter receive no significant contributions from particles beyond the Standard Model.

As reviewed below, one may parametrize the possible coupling deviations by coefficients a_V and c_f for vector bosons and fermions, respectively [51–54]. One possibility is that these coefficients are universal, i.e., $a_W = a_Z \equiv a$ and $c_t = c_b = c_\tau = c_c = \cdots \equiv c$, with the Standard Model corresponding to $a = c = 1$. There has been some speculation that custodial symmetry might be broken with $a_W \neq a_Z$ [55], and that couplings to some fermion species might be enhanced or suppressed. The present data are insufficient to probe these possibilities very precisely, and the overall quality of our global fit, presented below, indicates no need currently to adopt such hypotheses.

As already mentioned, a key prediction for the Standard Model Higgs boson is that its couplings to other particles are proportional to their masses. We probe this issue here by considering purely phenomenological parametrizations of the h couplings of the forms $a_V = v(M_V^{2\epsilon}/M^{(1+2\epsilon)})$ and $c_f = v(m_f{}^\epsilon/M^{1+\epsilon})$, where for a Standard Model Higgs boson $\epsilon = 0$ and $M = v = 246$ GeV, the canonical Higgs vacuum expectation value (vev), corresponding to $a = c = 1$.

Figures 1, 2, 3 and 4 display our main results. They quantify the extent to which the h particle walks like a Higgs and quacks like a Higgs.

Figure 1 shows the result in the (a, c) plane of our global fit to data on the h couplings from the Tevatron experiments and from the combined 7 and 8-TeV event samples of ATLAS and CMS. We see reasonable consistency with the Standard Model prediction: the overall best-fit region has $c > 0$ and, whilst the best fit has $a > 1$ and $c < 1$ (see also the marginalized one-dimensional likelihoods of our fit result projected on the a and c axes shown in figure 2), the Standard Model prediction lies within the 68% CL region. As we discuss in more detail below, figures 1 and 2 impose important constraints on composite Higgs models, disfavouring several such models unless their predictions resemble those of the Standard Model.

Figure 3 displays the result of our global fit in the (ϵ, M) plane, where we see excellent consistency with the Higgs hypothesis: $M = v, \epsilon = 0$. This is also seen in figure 4, which displays the marginalized one-dimensional likelihood projections of our fit result on the M and ϵ axes. The couplings of the h particle are clearly inconsistent with any mass-independent scenario, which would require $\epsilon = -1$. Figure 5 provides another way of understanding this observation. The points with vertical error bars represent the values of the h couplings to different particles found in our global fit to the parameters (ϵ, M). The diagonal dashed line is our best fit to (ϵ, M) and the dotted lines are given by the $\pm 1\sigma$ ranges in these parameters, as given in the upper legend of the plot. The solid red line in figure 5 represents the Standard Model prediction (2.6), which is compatible within errors with the measurements, as already discussed.

In subsequent sections we describe how these results were obtained, and present more details of our analysis. In section 2 we review the phenomenological frameworks we employ, and in section 3 we describe our calculational procedure, which follows closely that in [56]. In section 4 we describe the data set we use, focusing in particular on the recent update from the Tevatron experiments as well as the recent preliminary results from $\sim 5/\text{fb}$ of
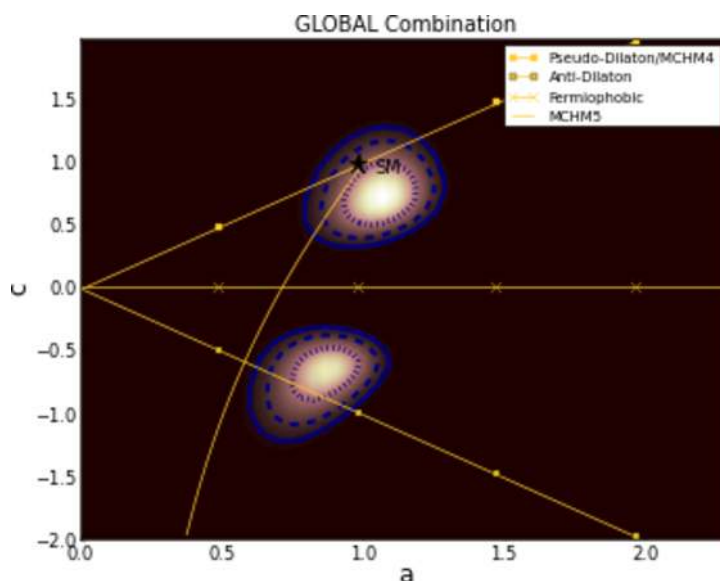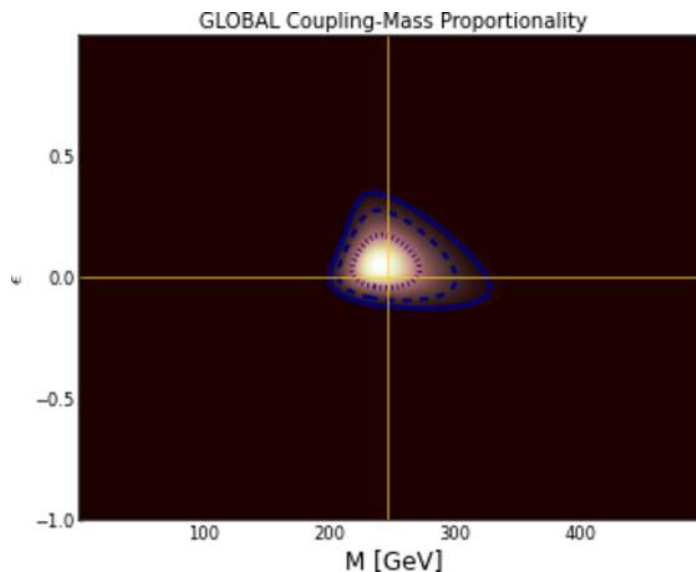
Figure 1. The constraints on the couplings (a, c) of the Higgs candidate h with mass $\sim 125\,\text{GeV}$ obtained from our global analysis of the available CMS, ATLAS, CDF and D0 data. The Standard Model is represented by a black star, and the yellow lines represent various composite Higgs models described in the text, which are disfavoured if they deviate strongly from the Standard Model. In these and subsequent analogous plots, the most likely regions have the lightest shading, the dotted lines are 68% CL contours, the dashed lines are 95% CL contours, and the solid lines are 99% CL contours.
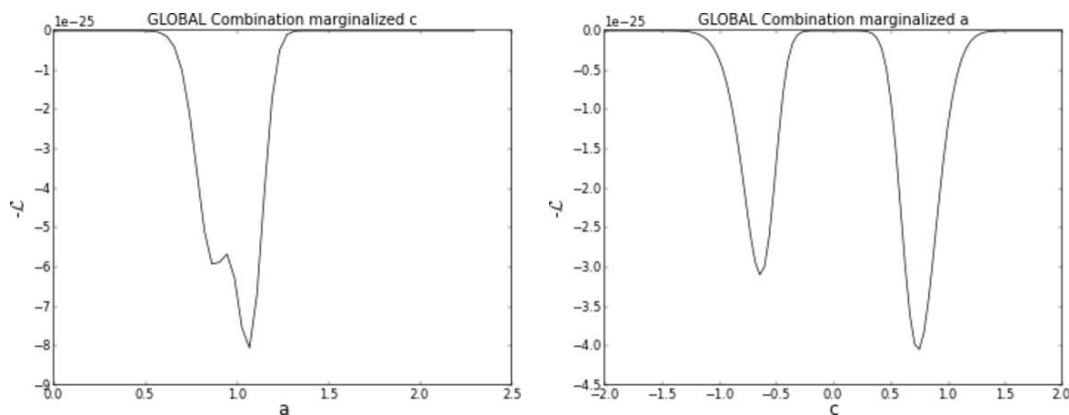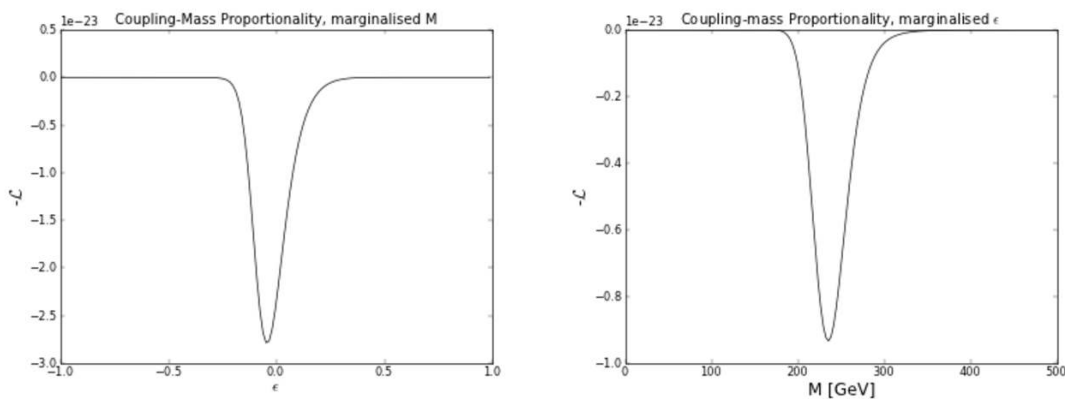

Figure 2. Marginalized one-dimensional projections on (left) the a and (right) the c axes of the likelihood function for our global fit result shown in figure 1.

8-TeV LHC data in each of ATLAS and CMS. In section 5 we present in more detail our results in the (a, c) plane, discussing their implications for pseudo-dilatons [57–72] and other composite Higgs scenarios [73, 74],[1] as well as fermiophobic (for a recent analysis see [78]) and gaugephobic [79] models. In section 6 we discuss in more detail our results in the (ϵ, M) plane, and in section 7 we present our conclusions and discuss the prospects that future data may soon clarify further the nature of the $\sim 125\,\text{GeV}$ Higgs candidate h.

---

[1]Radion models [75–77] are closely related.

Figure 3. The constraints on the scaling parameters (ϵ, M) of the Higgs candidate h with mass $\sim 125\,\text{GeV}$ obtained from our global analysis of the available CMS, ATLAS, CDF and D0 data. The Standard Model corresponds to the intersection of the yellow cross-hairs. The data are close to the 'bull's eye'.

Figure 4. Marginalized one-dimensional projections on (left) the ϵ and (right) M axes of the likelihood function for our global fit result shown in figure 3.

2 Phenomenological framework

We use the following nonlinear low-energy effective Lagrangian for the electroweak symmetry-breaking sector [51–54, 57–63], see also [80–85]:

$$
\begin{aligned}
\mathcal{L}_{\text{eff}} \;=\; & \frac{v^2}{4}\text{Tr}\left(D_\mu U D^\mu U^\dagger\right) \times \left[1 + 2a\frac{h}{v} + \dots\right] \\
& - \frac{v}{\sqrt{2}}\Sigma_f \bar{f}_L \lambda_f f_R \left[1 + c_f\frac{h}{v} + \dots\right] + h.c.
\end{aligned}
\tag{2.1}
$$

where U is a unitary 2×2 matrix parametrizing the three Nambu-Goldstone fields that
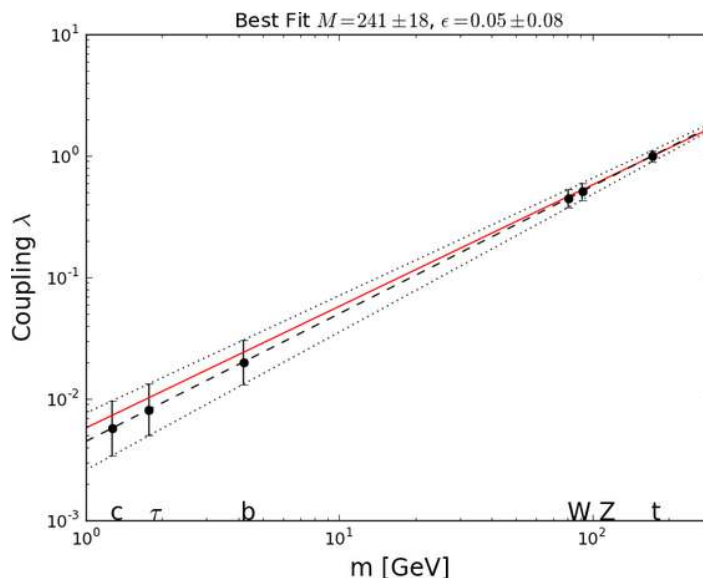
Figure 5. The mass dependence of the h couplings found in our (ϵ, M) fit. The vertical error bars correspond to the uncertainties shown in figure 4. The dashed line is our best fit, and the dotted lines correspond to $\pm 1\sigma$ variations in (ϵ, M). The Standard Model prediction that Higgs couplings should be proportional to the masses of other particles with $M = v$, shown by the diagonal solid red line, is completely consistent with the data.

are 'eaten' by the $W^\pm$ and Z^0, giving them masses, $v \sim 246\,\text{GeV}$ is the conventional electroweak symmetry-breaking scale, h is a field describing the Higgs candidate with mass $\sim 125\,\text{GeV}$ discovered by ATLAS and CMS, and λ_f is the Yukawa coupling of the fermion flavour f in the Standard Model. The coefficients a and c_f parametrize the deviations of the h couplings to massive vector bosons and to fermions, respectively, from those of the Higgs boson in the Standard Model. In writing (2.1), we have implicitly assumed a custodial symmetry: $a_W = a_Z = a$, an assumption whose plausibility can be judged from the overall quality of our fit.

Also relevant for the phenomenology of the Higgs candidate h are its dimension-5 loop-induced couplings to gg and $\gamma\gamma$ [86–89]:

$$\mathcal{L}_\Delta = -\left[\frac{\alpha_s}{8\pi} b_s G_{a\mu\nu} G_a^{\mu\nu} + \frac{\alpha_{em}}{8\pi} b_{em} F_{\mu\nu} F^{\mu\nu}\right]\left(\frac{h}{V}\right). \tag{2.2}$$

We assume here that, as in the Standard Model, only the top quark makes a significant contribution to the coefficient b_s, and only the top quark and the $W^\pm$ contribute significantly to b_{em} (with opposite signs in the Standard Model [86]).

We recall that, in a scenario in which h is associated with a pseudo-dilaton field χ with vev V, one has

$$a = c = \frac{v}{V}. \tag{2.3}$$

One may also consider scenarios in which h is a pseudo-Goldstone boson of some higher-order chiral symmetry that is broken down to the SU(2) × SU(2) of the Standard Model

Higgs sector. Among such composite models with an SO(5)/SO(4) structure [90–97], one may consider the MCHM4 option — in which the Standard Model fermions are embedded in spinorial representations of SO(5) and

$$a = c = \sqrt{1-\xi}, \tag{2.4}$$

where $\xi \equiv (v/f)^2$ with f a compositeness scale (which is equivalent to the pseudo-dilaton model with $v/V \to \sqrt{1-\xi}$), or the MCHM5 option — in which the Standard Model fermions are embedded in fundamental representations of SO(5) and

$$a = \sqrt{1-\xi} \,, \; c = \frac{1-2\xi}{\sqrt{1-\xi}}. \tag{2.5}$$

As discussed in [56], this interpolates between the Standard Model (obtained in the limit $\xi \to 0$), a specific fermiophobic scenario with $a = \sqrt{3}/2$ (obtained in the limit $\xi \to 1/2$), an 'anti-dilaton' model with $a = -c = 1/\sqrt{3}$ (obtained when $\xi = 2/3$), and a gaugephobic model (obtained when $\xi \to 1$).

In addition to these theoretically-motivated models, we also consider the completely phenomenological possibility that h couples to other particles proportionally to some power of their masses. Thus, we generalize the Standard Model couplings

$$\lambda_f = \sqrt{2}\frac{m_f}{v}, \; g_V = 2\frac{m_V^2}{v} \tag{2.6}$$

to the following forms of couplings with anomalous scaling laws:

$$\lambda_f = \sqrt{2}\left(\frac{m_f}{M}\right)^{1+\epsilon}, \; g_V = 2\left(\frac{m_V^{2(1+\epsilon)}}{M^{1+2\epsilon}}\right). \tag{2.7}$$

The Standard Model is recovered in the double limit $\epsilon \to 0, M \to v$, whereas the pseudo-dilaton/MCHM4 scenario would correspond to $\epsilon = 0$ and $M = V \neq v$, in general. In terms of the parameterization (2.1), the parametrizations (2.7) correspond to

$$c_f = v\left(\frac{m_f^\epsilon}{M^{1+\epsilon}}\right), \; a_V = v\left(\frac{M_V^{2\epsilon}}{M^{(1+2\epsilon)}}\right). \tag{2.8}$$

After presenting our global fits to the parameters a, c, we shall explore the extent to which the data already indicate that h couples to other particles proportionally to masses, i.e., with $\epsilon = 0$, and a normalization M similar to $v = 246\,\text{GeV}$.

3 Calculational procedure

Assuming that the Higgs candidate h has no non-standard production or decay modes, its production cross-sections and decay widths are related to those of the Standard Model Higgs boson by simple factors of a and c. Assuming that gluon-gluon fusion (gg) and vector-boson fusion (VBF) dominate over the other processes, as at the LHC, one may combine

channel	Production sensitive to		Decay sensitive to	
	a	c	a	c
$\gamma\gamma$	✓	✓	✓	✓
$\gamma\gamma$ VBF	✓	✗	✓	✓
WW	✓	✓	✓	✗
WW 2-jet	✓	✗	✓	✗
WW 0,1-jet	✗	✓	✓	✗
$b\bar{b}$ (VH)	✓	✗	✗	✓
$b\bar{b}$ ($\bar{t}tH$)	✗	✓	✗	✓
ZZ	✓	✓	✓	✗
$\tau\tau$	✓	✓	✗	✓
$\tau\tau$ (VBF, VH)	✓	✗	✗	✓

Table 1. The dominant dependences on the model parameters (a, c) (2.1) of the h detection and search channels discussed in this paper, adapted from [56].

their respective production rescaling factors $R \equiv \sigma/\sigma_{\mathrm{SM}}$ and cut efficiencies $\xi_{\mathrm{gg,VBF}}$ to obtain a total production rescaling factor

$$R_{\mathrm{prod}} = \frac{\xi_{gg}F_{gg}R_{gg} + \xi_{\mathrm{VBF}}(1 - F_{gg})R_{\mathrm{VBF}}}{\xi_{gg}F_{gg} + \xi_{\mathrm{VBF}}(1 - F_{gg})} \quad , \tag{3.1}$$

where $F_{gg} \equiv \sigma_{gg}^{\mathrm{SM}}/\sigma_{\mathrm{tot}}^{\mathrm{SM}}$. In the case of the Tevatron, where associated production (AP) is more important that VBF, one may use (3.1) with the replacement VBF $\to$ AP throughout. For the CMS diphoton subchannels, the collaboration provides a full breakdown of the percentage contribution from all production mechanisms which can be used directly instead of the $\xi_i F_i$ factors above.

Similarly, relative to the Standard Model predictions, the decay widths $R \equiv \Gamma/\Gamma_{\mathrm{SM}}$ to massive vector bosons, fermions and photons are given, respectively, by

$$R_{VV} = a^2 \quad , \quad R_{\bar{f}f} = c^2 \quad , \quad R_{\gamma\gamma} = \frac{(-\frac{8}{3}cF_t + aF_w)^2}{(-\frac{8}{3}F_t + F_w)^2} \quad , \tag{3.2}$$

where the loop factors $F_{t,w}$ were given, e.g., in [56]. The principal dependences of the different Higgs-like signals on the rescaling factors (a, c) are summarized in table 1, which is adapted from [56]. It is important to emphasize that, since production mechanisms are in general also sensitive to both a and c, as well as decay branching ratios, their dependences also provide important constraints on model parameters.

The signal strength modification factor $\mu^i \equiv n_s^i/(n_s^i)^{\mathrm{SM}}$ in any given channel i is the product of the production and decay rescalings: $R \equiv R_{\mathrm{prod}}^i \cdot (R_{\mathrm{decay}}^i/R_{\mathrm{tot.}})$. In the absence of more detailed experimental information, we follow [98] as in [56], assuming that in each

channel the underlying likelihood $p(n_{\rm obs}|\mu n_s^{\rm SM} + n_b)$ obeys a Poisson distribution, and use the approximation $\sigma_{\rm obs} \simeq \sigma_{\rm exp} = \mu_{\rm exp}^{95\%}/1.96$ for the standard deviation to solve for the central value $\bar{\mu}$ in the equation:

$$\frac{\int_0^{\mu^{95\%_{\rm obs}}} e^{-\frac{(\mu-\bar{\mu})^2}{2\sigma_{\rm obs}^2}}\, d\mu}{\int_0^\infty e^{-\frac{(\mu-\bar{\mu})^2}{2\sigma_{\rm obs}^2}}\, d\mu} = 0.95 \quad . \tag{3.3}$$

The posterior probability density function is then given by

$$p(\mu|n_{\rm obs}) = p(n_{\rm obs}|\mu n_s^{\rm SM} + n_b) \cdot \pi(\mu) \approx \frac{1}{\sqrt{2\pi\sigma_{\rm obs}^2}} e^{-\frac{(\mu-\bar{\mu})^2}{2\sigma_{\rm obs}^2}} \quad , \tag{3.4}$$

with $\pi(\mu)$ generally assumed *a priori* to be flat within the range of interest and zero outside.

4 Experimental data set

We use the latest available information from ~ 5/fb of LHC data obtained at each of 7 and 8 TeV in the centre of mass presented at ICHEP 2012 [15–18], and ~ 10/fb of Tevatron data analyzed in [29, 30]. In addition to [15, 16], the CMS Collaboration provides additional information on its 7 and 8 TeV fits separately in public analysis notes, see below.

1. The CMS and ATLAS searches in the channel $h \to ZZ \to 4\ell^\pm$ are treated as inclusive for both 7 and 8 TeV [3, 4, 19, 25].

2. The searches in the $h \to \bar{b}b$ VH channel are assumed to be dominated by associated production, with the Tevatron data updated from [56] to the latest results in [29, 30], the 7 TeV Moriond results are used for ATLAS [5], and the CMS 7 and 8 TeV fits are obtained from [19]. In addition the CMS 7 TeV $\bar{t}tH$ channel is included from [24].

3. The diphoton likelihoods in the ATLAS searches at 7 TeV were obtained from [7] as explained in [56]. In [20] CMS provides central values and one sigma error bars for both 7 and 8 TeV searches in four inclusive sub-channels dominated by gluon fusion and one or two di-jet categories. We treat the 8 TeV ATLAS results inclusively since the sub-channel best fit values are only provided for $m_h = 126.5$ [26].[2] The Tevatron search from [29, 30] are also included.

4. The Tevatron results for $h \to W^+W^-$ are updated from [29, 30]. The corresponding ATLAS results for 7 TeV [8] are supplemented by the 8 TeV data made public recently in [27]. CMS provide fits in the 0,1 and 2-jet categories for both 7 and 8 TeV [19, 22].

5. The ATLAS $\tau\tau$ searches at 7 TeV are treated as inclusive [10]. For CMS we use the best fits provided for the 0,1-jet and VBF channels at 7 and 8 TeV in [19, 23]. At 7 TeV there is also an additional CMS search in the VH channel.

---

[2]As discussed below, our results are quite insensitive to the assumed for h in the range $[124, 127]$ GeV.

As mentioned in the previous section, we use in our fit the CMS information on the percentage contribution from each production mechanism for all the diphoton sub-categories at 7 and 8 TeV separately. We treated the $\tau\tau$ VBF categories assuming $\sim$30% contamination from gluon fusion in the production mechanism. As mentioned in [56], we expect that our global analysis is only accurate to $\sim$20% due to the limited experimental information available so far [99].

5 Results

5.1 Tevatron data

We consider first the fit to the recent Tevatron data in terms of (a, c) that is shown in figure 6. We recall that the Tevatron experiments CDF and D0 provide information on the associated production (AP) of h followed by its decay into $\bar{b}b$ (upper left panel of figure 6), as well as inclusive measurements of $h \to WW^*$ decay (upper right panel) and now also $h \to \gamma\gamma$ decay (lower left panel). The central value of the $h \to \bar{b}b$ signal is somewhat stronger than expected in the Standard Model, disfavouring fermiophobic models and corresponding to the possibility that either a and/or $c > 1$. However, the Tevatron $h \to WW^*$ signal is relatively weak, disfavouring large a. The $h \to \gamma\gamma$ signal is relatively strong, but very uncertain. In combination (lower right panel of figure 6), the Tevatron data are compatible with the Standard Model, while favouring slightly $a, c > 1$.

5.2 CMS data

We now turn to the analysis of the ICHEP 2012 CMS data shown in figure 7. The $h \to \bar{b}b$ search (top left panel) was based on AP and $\bar{t}t$ Higgsstrahlung (HS) event selections, the former being more sensitive. The overall signal strength is somewhat below that expected in the Standard Model, slightly favouring $a, c < 1$, but very compatible with the Standard Model. The $h \to \tau^+\tau^-$ search (top right panel) was based on a combination of event selections favouring gluon-gluon fusion, VBF and AP production mechanisms. Once again the overall signal is weaker than expected in the Standard Model, but not very significantly. The $h \to ZZ^*$ signal (middle left panel) has the strength expected in the Standard Model, disfavouring $a \ll 1$. The $h \to WW^*$ search shown in the middle right panel of figure 7 was based on a combination of event selections favouring gluon-gluon fusion and VBF production mechanisms, and the deficit compared to the Standard Model is not very significant. Finally, the $h \to \gamma\gamma$ event selection includes samples with and without enhanced VBF contributions. As discussed in [56], since the $h \to \gamma\gamma$ decay amplitude contains both t and W loops, which interfere, it provides unique discrimination between the cases $a >$ and < 0, as seen in the bottom left panel of figure 7. Although the $\gamma\gamma$ signal strength is somewhat stronger than in the Standard Model, particularly in the VBF-enhanced sample, the discrepancy is not highly significant. Turning now to the overall combination of CMS data shown in the bottom right panel of figure 7, we see that the overall best fit is in a region with $c < 1$, driven by the $\gamma\gamma$ channel. The favoured region with $c > 0$ is compatible
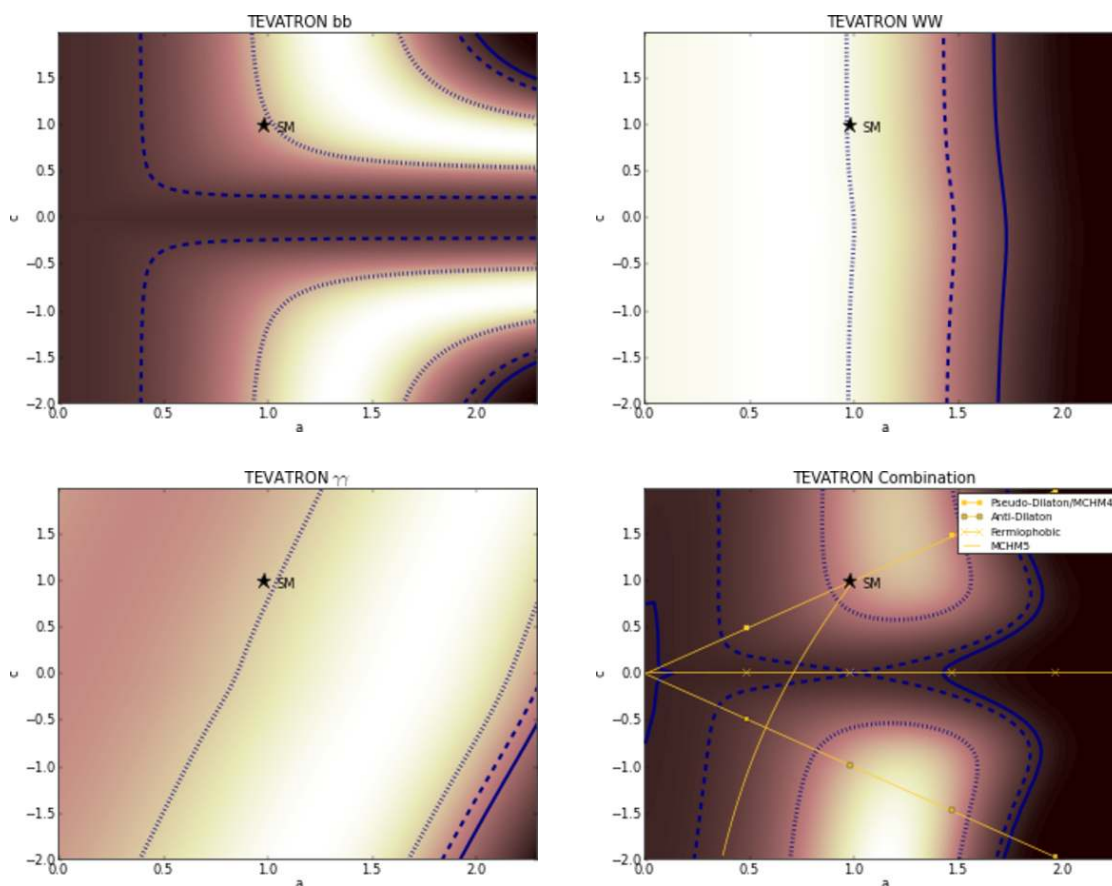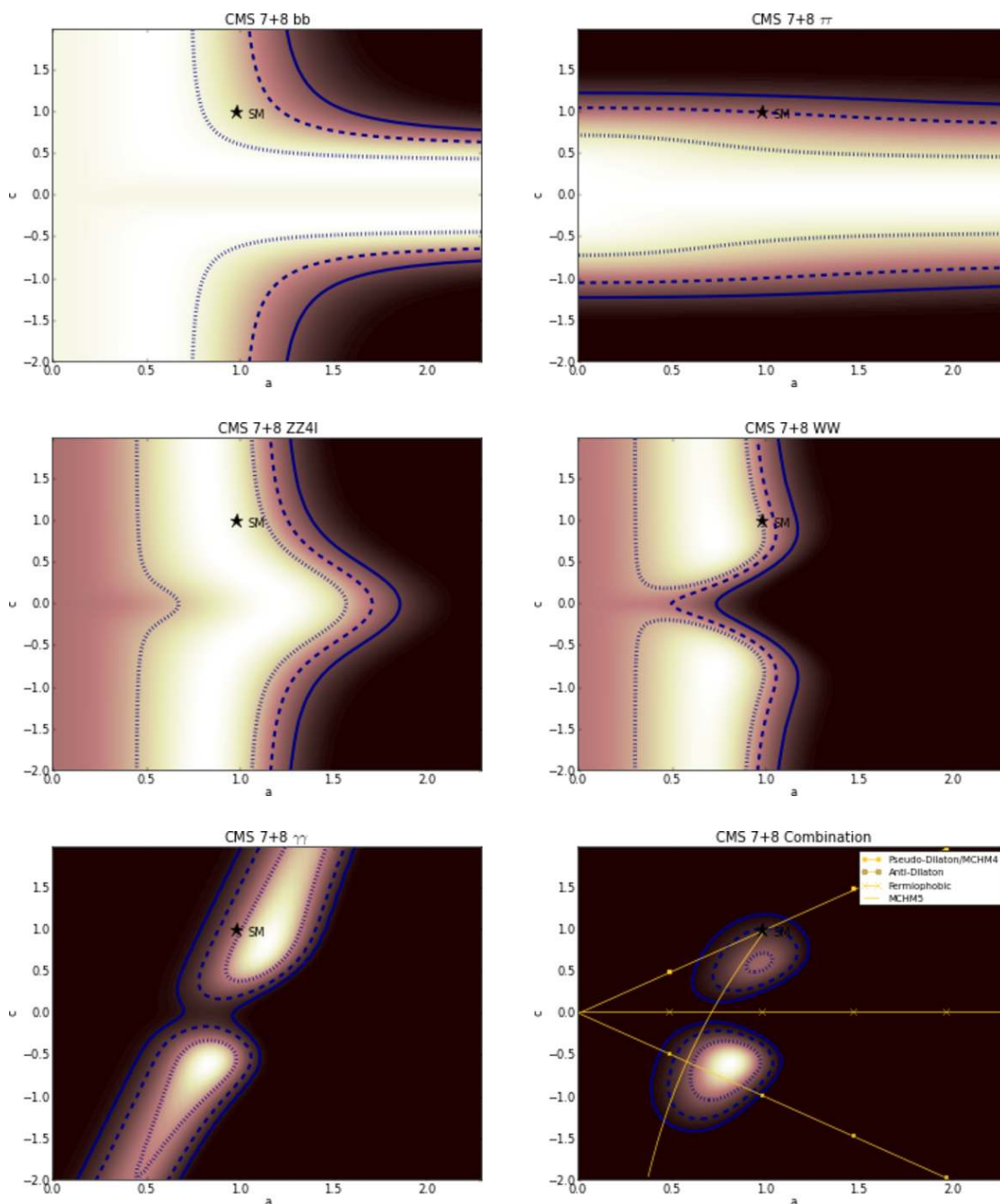
Figure 6. Constraints on the couplings (a, c) of the Higgs candidate h with mass $\sim 125\,\mathrm{GeV}$ arising from the CDF and D0 data on (upper left) $\bar{b}b$, (upper right) $\tau^{+}\tau^{-}$, and (lower left) $\gamma\gamma$ final states. The lower right panel displays the combination of these ICHEP 2012 CMS constraints, together with lines representing the pseudo-dilaton/MCHM4, anti-dilaton, fermiophobic and MCHM5 scenarios.

with the Standard Model, with $a \sim 1$ though $c < 1$ is somewhat favoured.[3] Comparing with the analogous panel in figure 1 of [56], we see that the accuracy in the determination of the h couplings has improved significantly.

5.3 ATLAS data

We now present a similar analysis of the available ATLAS data, which yields the results shown in figure 8. As in the previous figure, the top left panel displays the constraint in the (a, c) plane provided by the $h \to \bar{b}b$ search, which in the ATLAS case is based on $\sim 5/\mathrm{fb}$ of data at 7 TeV, as is the $h \to \tau^{+}\tau^{-}$ constraint shown in the top right panel of figure 8. These panels are the same as the corresponding panels in figure 5 of [56]. The middle left panel of figure 8 displays the $h \to ZZ^{*}$ constraint including also $\sim 5/\mathrm{fb}$ of data at 8 TeV: we see that the central value of the signal strength lies somewhat above the value expected

---

[3]When we restrict our fit to $c > 0$, we obtain a result very similar result to that reported by the CMS Collaboration [15, 16].

Figure 7. Constraints on the couplings (a, c) of the Higgs candidate h with mass $\sim 125\,\text{GeV}$ arising from the ICHEP 2012 CMS data on (top left) $\bar{b}b$, (top right) $\tau^+\tau^-$, (centre left) ZZ^*, (centre right) WW^* and (bottom left) $\gamma\gamma$ final states. The bottom right panel displays the combination of these ICHEP 2012 CMS constraints, together with lines representing the pseudo-dilaton/MCHM4, anti-dilaton, fermiophobic and MCHM5 scenarios. As in other analogous plots, the most likely regions have the lightest shading, the dotted lines are 68% CL contours, the dashed lines are 95% CL contours, and the solid lines are 99% CL contours.

in the Standard Model, corresponding to $a > 1$. The central value of the $h \to WW^*$ signal shown in the middle right panel of figure 8 (which is based on $\sim 5/$fb of data each at 7 TeV and 8 TeV) has $a > 1$, but is consistent with $a = 1$ at the 68% CL. Finally, the combined ATLAS 7- and 8-TeV search for $h \to \gamma\gamma$ shown in the bottom right panel of figure 8 yields a central value of the strength lying somewhat above the Standard Model value, which is reflected in the preferred region of the (a, c) plane. The overall combination of the available ATLAS constraints, shown in the bottom right panel, indicates a general preference for $a > 0$, with values of $a > 1, c < 1$ being favoured.

6 Combined results in the (a, c) plane and implications for models

Looking at the bottom right panels of figures 6, 7 and 8, the general features of figure 1 can now be understood. Since they do not have high sensitivity to $h \to \gamma\gamma$, the Tevatron data are unable to discriminate between the upper and lower halves of the (a, c) plane. The CMS data do have high sensitivity to $h \to \gamma\gamma$, leading to some asymmetry between the upper and lower halves of the (a, c) plane, with a preference for $c < 0$. On the other hand, the ATLAS $h \to \gamma\gamma$ and WW^* data provide some preference for $c > 0$. Generally speaking, the Tevatron data prefer $a, c > 1$, whereas the CMS and ATLAS data prefer $a > 1$ and $c < 1$. The overall result, shown in figure 2, is that the global combination prefers $a > 1$ (left panel) and $c > 0$ (right panel), though not very significantly, and the favoured region with $c > 0$ has a slightly > 1 (left panel) and c slightly < 1 (right panel).

The absence of strong $\bar{b}b$ and $\tau^+\tau^-$ signals at the LHC favours speculation that $c \ll 1$, but in models with a universal coefficient c for all fermions, this is not the whole story. The fact the total h cross section is compatible with the Standard Model indicates that the $h\bar{t}t$ couplings should be close to the Standard Model value, corresponding to $c \sim 1$. Moreover, the Tevatron experiments report evidence for a strong $\bar{b}b$ decay signal, and as this is the dominant decay mode in the Standard Model the whole pattern of h decays would be very different if $c \ll 1$. The right panel of figure 2 is the net result: no significant discrepancy with the Standard Model if c is universal.

Likewise, the absence of a strong $h \to WW^*$ signal in the Tevatron, CMS and the ATLAS 7-TeV data might have led one to speculate that $a < 1$, or even that $a_W \neq a_Z$ with custodial symmetry broken [55]. However, the fact that the $h \to \gamma\gamma$ signals reported by both ATLAS and CMS are on the high side suggests that the $h\gamma\gamma$ loop amplitude in (3.2) must receive an important contribution from the $W^\pm$ loops, which should be dominant. This and the ATLAS 8-TeV data suggest that a_W cannot be very small, and favours $a \equiv a_W = a_Z$ not ~ 1 in our fit.

We display in figure 1 yellow lines corresponding to the predictions of the pseudo-dilaton and MCHM4 models (2.3), (2.4) ($a = c = v/V, \sqrt{1 - \xi}$), 'anti-dilaton' models ($a = -c$), the MCHM5 model (2.5) ($a = \sqrt{1 - \xi}, c = (1 - 2\xi/\sqrt{1 - \xi})$), fermiophobic models ($c = 0$) and gaugephobic models ($a = 0$).[4] We see in the right panel of figure 4 that models with an overall scale M similar to the value $v = 246$ GeV in the Standard Model

---

[4]See also the combination panels in figures 6, 7 and 8 for the corresponding individual comparisons with Tevatron, CMS and ATLAS data, respectively.
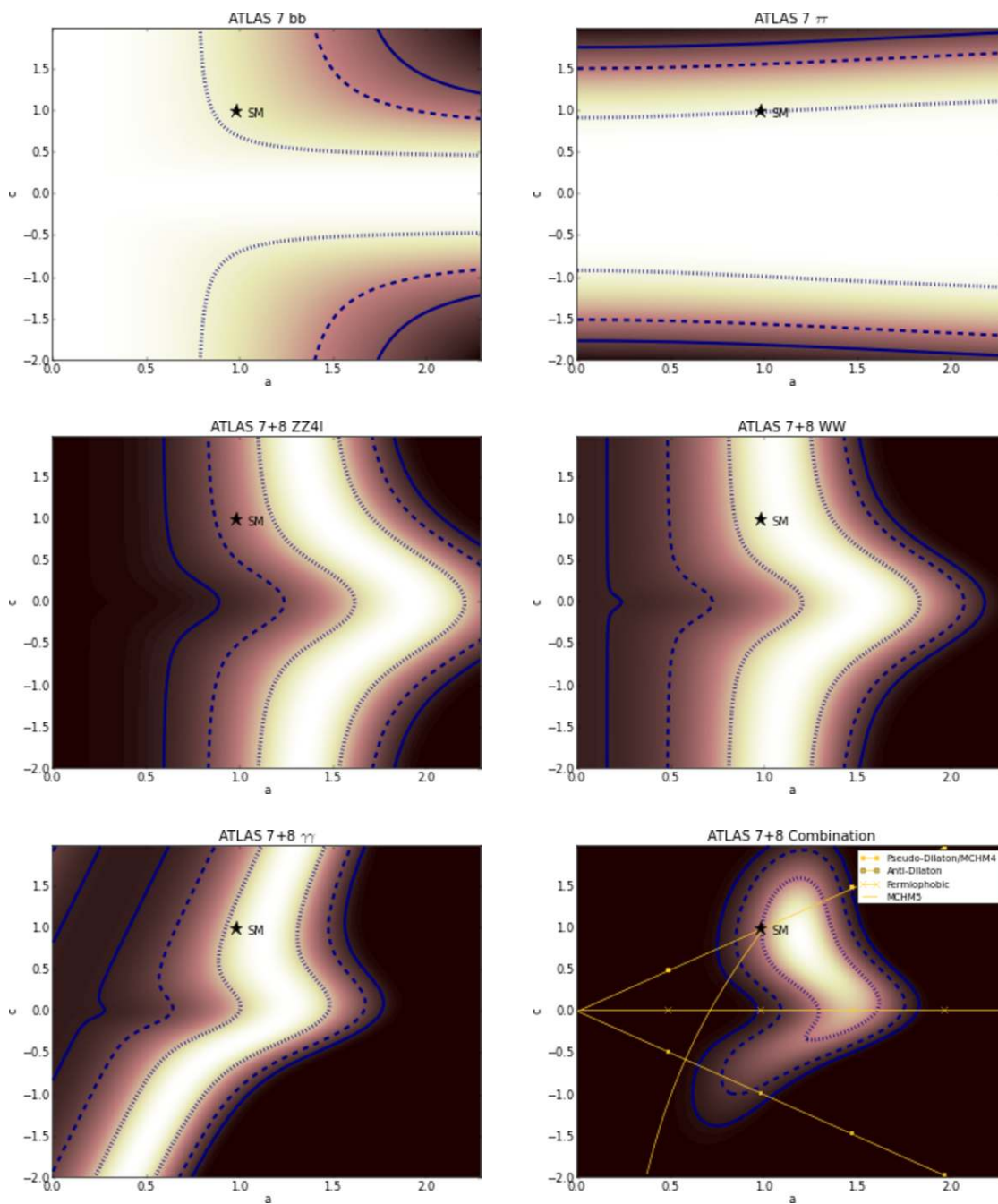
Figure 8. Constraints on the couplings (a, c) of the Higgs candidate h with mass $\sim 125\,\mathrm{GeV}$ arising from the ATLAS data on (top left) $\bar{b}b$, (top right) $\tau^+\tau^-$, (centre left) ZZ^*, (centre right) WW^* and (bottom left) $\gamma\gamma$ final states. The bottom right panel displays the combination of these ICHEP 2012 ATLAS constraints, together with lines representing the pseudo-dilaton/MCHM4, anti-dilaton, fermiophobic and MCHM5 scenarios.

are strongly favoured. These correspond to the cases $V \sim v$ in pseudo-dilaton models and $\xi \sim 0$ in the MCHM4 model. However, in pseudo-dilaton models, in particular, there may be additional heavy particles contributing to the loop coefficients b_s, b_{em} in (2.2) [64–72], so this observation is model-dependent and further analysis is needed [100, 101]. We also see in figure 1 that the $\xi \to 0$ limit of the MCHM5 model is preferred, while 'anti-dilaton' models are slightly disfavoured compared to pseudo-dilaton models, and would prefer $a = -c < 1$: see also the right panel of figure 2. Finally, we observe that the fermiophobic and gaugephobic models are strongly disfavoured.

7 Combined results in the (ϵ, M) plane

The h particle is clearly very different from any other known 'fundamental' particle. The fact that it decays into $\gamma\gamma$ implies that it cannot have spin one, and hence cannot be a gauge boson. It may well have spin zero: this remains to be demonstrated, though this hypothesis has been used in the WW^* and ZZ^* event selections. If it has spin 2, that would make it an even more remarkable discovery. If it does have spin zero, there is no reason why its couplings to different fermion generations (for example) should be universal, and the Higgs hypothesis suggests that its couplings to other particles should be proportional to their masses.

We now discuss the light on the nature of the h particle that is cast by figures 3, 4 and 5. In particular, figure 3 suggests that the data are heading straight towards the Higgs 'bull's eye' at the cross-hairs where $M \sim v = 246\,\text{GeV}$ and $\epsilon \sim 0$, corresponding to couplings scaling with masses. As we see in the right panel of figure 4, the hypothesis $M = v$ is indeed favoured. The left panel of figure 4 tells us that small values of ϵ are also favoured, and the Higgs hypothesis $\epsilon = 0$ is quite compatible with the available data. Our global fit yields

$$\epsilon \; = \; 0.05 \pm 0.08, \;\; M \; = \; 241 \pm 18 \text{ GeV}. \tag{7.1}$$

At first sight, one might be surprised that it is already possible to obtain such a tight constraint on ϵ. The essential reason is that, because it is so much heavier than all the other fermions, the coupling to the top quark provides a long lever arm, and similarly for the $W^\pm$ and Z because they are also much heavier than the other fermions. As already commented in section 1, figure 5 provides another way of visualizing this observation. The diagonal line in figure 5 that represents the mass dependence of the Higgs couplings expected in the Standard Model (2.6) is completely compatible within errors with the measurements.

We consider figures 3, 4 and 5 to be the most remarkable results of our analysis.

8 Overview and prospects

A new particle has been discovered: how closely does it resemble the Higgs boson of the Standard Model? In this paper we have presented a global analysis of the data from the Tevatron experiments [29, 30] CDF, D0, ATLAS [17, 18] and CMS [15, 16] made available before the ICHEP 2012 conference, making two types of fit. One is in terms of universal coefficients (a, c) that parametrize the deviations of the h couplings to fermions and bosons
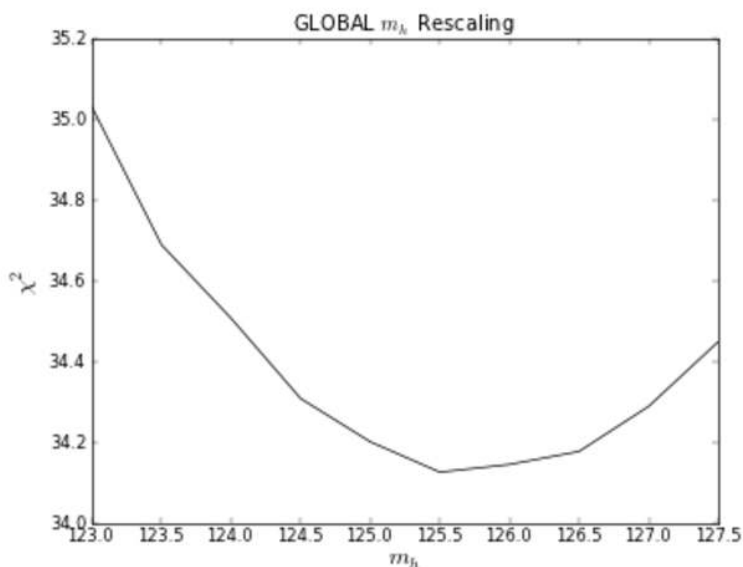
Figure 9. The overall χ^2 of a global fit to the available CDF, D0, ATLAS and CMS data as a function of m_h, obtained by calculating the h production cross-sections and decay branching rates assuming Standard Model couplings, but not including information on the shapes of the h signal in, e.g., the high-resolution $\gamma\gamma$ and ZZ^* channels as functions of m_h.

in a way well adapted to constraining composite Higgs models such as the pseudo-dilaton, MCHM4 and MCHM5 models, as well as the 'anti-dilaton', fermiophobic and gaugephobic scenarios. As seen in figures 1 and 2, the only models favoured in this fit are pseudo-dilaton and MCHM4 models with parameters close to the Standard Model case. We have also made a fit with h couplings to fermions and bosons scaling as some power $1 + \epsilon$ of the particle masses, with a normalization scale $M \neq v$ in general. As seen in figures 3, 4 and 5, this fit favours $\epsilon \sim 0$ and $M \sim v$, as expected for the Standard Model Higgs boson.

As seen in figure 9, the overall quality of a fit to the Standard Model Higgs boson is good, and does not depend strongly on m_h. This plot was made by calculating the h production cross-sections and decay branching rates assuming Standard Model couplings, i.e., $a = c = 1, \epsilon = 0, M = v$, while leaving m_h as a free parameter. Note that information on the shapes of the h signal in, e.g., the high-resolution $\gamma\gamma$ and ZZ^* channels as functions of m_h was not used in this exercise. The value of the global χ^2 function at the minimum, namely 34.1, is comparable to the number of degrees of freedom in the fit. Better understanding of the correlations in the data are needed, but the overall quality of the Standard Model Higgs fit is clearly good. We also see in figure 9 that the quality of this fit does not vary significantly over the range $[124, 127]$ GeV, which brackets the central values of m_h found in the high-resolution $\gamma\gamma$ and ZZ^* channels by CMS and ATLAS. Within this range, our other results are insensitive to the value $m_h = 125$ GeV assumed in our global fits.

We anticipate that the LHC experiments will be able to constrain the h couplings significantly further in the coming months, with improved analyses of the channels already studied, analyses of more channels using the data accumulated so far, and the prospect

of more data on the way. We expect that these improvements will enable the ranges of parameters in simple two-parameter fits such as those presented here to be reduced to the 10% level [102–106]. The upcoming data should also make possible more detailed fits incorporating more parameters, leading eventually to individual determinations of the h couplings to different bosons and fermions. In this way, we shall see whether the indication of h couplings depending linearly on other particle masses seen in figures 3, 4 and 5 will be confirmed.

So far, the h particle does indeed walk and quack very much like a Higgs boson.

Acknowledgments

Open Access. This article is distributed under the terms of the Creative Commons Attribution License which permits any use, distribution and reproduction in any medium, provided the original author(s) and source are credited.

References

[1] ATLAS collaboration, G. Aad et al., *Combined search for the standard model Higgs boson using up to 4.9 fb^{-1} of pp collision data at $\sqrt{s} = 7$ TeV with the ATLAS detector at the LHC, Phys. Lett.* **B 710** (2012) 49 [arXiv:1202.1408] [INSPIRE].

[2] CMS collaboration, S. Chatrchyan et al., *Combined results of searches for the standard model Higgs boson in pp collisions at $\sqrt{s} = 7$ TeV, Phys. Lett.* **B 710** (2012) 26 [arXiv:1202.1488] [INSPIRE].

[3] CMS collaboration, S. Chatrchyan et al., *Search for the standard model Higgs boson in the decay channel $H \to ZZ \to 4$ leptons in pp collisions at $\sqrt{s} = 7$ TeV, Phys. Rev. Lett.* **108** (2012) 111804 [arXiv:1202.1997] [INSPIRE].

[4] ATLAS collaboration, G. Aad et al., *Search for the standard model Higgs boson in the decay channel $H \to ZZ^{(*)} \to 4l$ with 4.8 fb^{-1} of pp collision data at $\sqrt{s} = 7$ TeV with ATLAS, Phys. Lett.* **B 710** (2012) 383 [arXiv:1202.1415] [INSPIRE].

[5] ATLAS collaboration, *Search for the standard model Higgs boson produced in association with a vector boson and decaying to a b-quark pair using up to 4.7 fb^{-1} pp collision data at $\sqrt{s} = 7$ TeV with the ATLAS detector at the LHC,* ATLAS-CONF-2012-015 (2012).

[6] CMS collaboration, *A search using multivariate techniques for a standard model Higgs boson decaying into two photons,* CMS-HIG-PAS-12-001 (2012).

[7] ATLAS collaboration, G. Aad et al., *Search for the standard model Higgs boson in the diphoton decay channel with 4.9 fb^{-1} of pp collisions at $\sqrt{s} = 7$ TeV with ATLAS, Phys. Rev. Lett.* **108** (2012) 111803 [arXiv:1202.1414] [INSPIRE].

[8] ATLAS collaboration, *Search for the Standard Model Higgs boson in the $H \to WW \to \ell\nu\ell\nu$ decay mode with 4.7 fb^{-1} of ATLAS data at $\sqrt{s} = 7$ TeV,* ATLAS-CONF-2012-012 (2012).

[9] CMS collaboration, S. Chatrchyan et al., *Search for the standard model Higgs boson decaying to a W pair in the fully leptonic final state in pp collisions at $\sqrt{s} = 7$ TeV*, *Phys. Lett.* **B 710** (2012) 91 [arXiv:1202.1489] [INSPIRE].

[10] ATLAS collaboration, *Search for the standard model Higgs boson in the $H \to \tau^+\tau^-$ decay mode with 4.7 fb^{-1} of ATLAS data at 7 TeV*, ATLAS-CONF-2012-014 (2012).

[11] CMS collaboration, *Search for neutral Higgs bosons decaying into τ leptons in the dimuon channel with CMS in pp collisions at 7 TeV*, CMS-PAS-HIG-12-007 (2012).

[12] CMS collaboration, *Search for WH to 3 leptons*, CMS-PAS-HIG-11-034 (2011).

[13] CMS collaboration, *Search for WH in final states with electrons, muons, taus*, CMS-PAS-HIG-12-006 (2012).

[14] CMS collaboration, S. Chatrchyan et al., *Search for the standard model Higgs boson decaying into two photons in pp collisions at $\sqrt{s}=7$ TeV*, *Phys. Lett.* **B 710** (2012) 403 [arXiv:1202.1487] [INSPIRE].

[15] CMS collaboration, S. Chatrchyan et al., *Observation of a new boson at a mass of 125 GeV with the CMS experiment at the LHC*, *Phys. Lett.* **B 716** (2012) 30 [arXiv:1207.7235] [INSPIRE].

[16] CMS collaboration, J. Incandela, *Status of the CMS SM Higgs search*, talk given at *CERN Seminar*, July 4, CERN, Switzerland (2012).

[17] ATLAS collaboration, G. Aad et al., *Observation of a new particle in the search for the Standard Model Higgs boson with the ATLAS detector at the LHC*, *Phys. Lett.* **B 716** (2012) 1 [arXiv:1207.7214] [INSPIRE].

[18] ATLAS collaboration, F. Gianotti, *Status of standard model Higgs searches at ATLAS*, talk given at *CERN Seminar*, July 4, CERN, Switzerland (2012).

[19] CMS collaboration, *Observation of a new boson with a mass near 125 GeV*, CMS-PAS-HIG-12-020 (2012).

[20] CMS collaboration, *Evidence for a new state decaying into two photons in the search for the standard model Higgs boson in pp collisions*, CMS-PAS-HIG-12-015 (2012).

[21] CMS collaboration, *Evidence for a new state in the search for the standard model Higgs boson in the $H \to ZZ \to 4$ leptons channel in pp collisions at $\sqrt{s} = 7$ and 8 TeV*, CMS-PAS-HIG-12-016 (2012).

[22] CMS collaboration, *Search for the standard model Higgs boson decaying to a W pair in the fully leptonic final state in pp collisions at $\sqrt{s} = 8$ TeV*, CMS-PAS-HIG-12-017 (2012).

[23] CMS collaboration, *Search for a standard model Higgs bosons decaying to τ pairs in pp collisions*, CMS-PAS-HIG-12-018 (2012).

[24] CMS collaboration, *Search for Higgs boson production in association with top quark pairs in pp collisions*, CMS-PAS-HIG-12-025 (2012).

[25] ATLAS collaboration, *Observation of an excess of events in the search for the Standard Model Higgs boson in the $H \to ZZ^{(*)} \to 4\ell$ channel with the ATLAS detector.*, ATLAS-CONF-2012-092 (2012).

[26] ATLAS collaboration, *Observation of an excess of events in the search for the standard model Higgs boson in the γ-γ channel with the ATLAS detector*, ATLAS-CONF-2012-091 (2012).

[27] ATLAS collaboration, *Observation of an Excess of Events in the Search for the Standard Model Higgs Boson in the $H \to WW^{(*)} \to \ell\nu\ell\nu$ Channel with the ATLAS Detector*, ATLAS-CONF-2012-098 (2012).

[28] ATLAS collaboration, *Observation of an excess of events in the search for the standard model Higgs boson with the ATLAS detector at the LHC*, ATLAS-CONF-2012-093 (2012).

[29] CDF, D0 collaboration, T. Aaltonen et al., *Evidence for a particle produced in association with weak bosons and decaying to a bottom-antibottom quark pair in Higgs boson searches at the Tevatron*, *Phys. Rev. Lett.* **109** (2012) 071804 [arXiv:1207.6436] [INSPIRE].

[30] TEVATRON NEW PHYSICS HIGGS WORKING GROUP, CDF, D0 collaboration, *Updated combination of CDF and D0 searches for standard model Higgs boson production with up to $10.0\,fb^{-1}$ of data*, arXiv:1207.0449 [INSPIRE].

[31] F. Englert and R. Brout, *Broken symmetry and the mass of gauge vector mesons*, *Phys. Rev. Lett.* **13** (1964) 321 [INSPIRE].

[32] P.W. Higgs, *Broken symmetries and the masses of gauge bosons*, *Phys. Rev. Lett.* **13** (1964) 508 [INSPIRE].

[33] P.W. Higgs, *Broken symmetries, massless particles and gauge fields*, *Phys. Lett.* **12** (1964) 132 [INSPIRE].

[34] G. Guralnik, C. Hagen and T. Kibble, *Global conservation laws and massless particles*, *Phys. Rev. Lett.* **13** (1964) 585 [INSPIRE].

[35] P.W. Higgs, *Spontaneous symmetry breakdown without massless bosons*, *Phys. Rev.* **145** (1966) 1156 [INSPIRE].

[36] T. Kibble, *Symmetry breaking in non-abelian gauge theories*, *Phys. Rev.* **155** (1967) 1554 [INSPIRE].

[37] J. Ellis and D.S. Hwang, *Does the 'Higgs' have spin zero?*, arXiv:1202.6660 [INSPIRE].

[38] J. Espinosa, C. Grojean, M. Muhlleitner and M. Trott, *Fingerprinting Higgs Suspects at the LHC*, *JHEP* **05** (2012) 097 [arXiv:1202.3697] [INSPIRE].

[39] P.P. Giardino, K. Kannike, M. Raidal and A. Strumia, *Reconstructing Higgs boson properties from the LHC and Tevatron data*, *JHEP* **06** (2012) 117 [arXiv:1203.4254] [INSPIRE].

[40] T. Li, X. Wan, Y.-k. Wang and S.-h. Zhu, *Constraints on the universal varying Yukawa couplings: from SM-like to fermiophobic*, arXiv:1203.5083 [INSPIRE].

[41] M. Rauch, *Determination of Higgs-boson couplings (SFitter)*, arXiv:1203.6826 [INSPIRE].

[42] J.R. Espinosa, M. Muhlleitner, C. Grojean and M. Trott, *Probing for invisible Higgs decays with global fits*, arXiv:1205.6790 [INSPIRE].

[43] I. Low, J. Lykken and G. Shaughnessy, *Have we observed the Higgs (imposter)?*, arXiv:1207.1093 [INSPIRE].

[44] T. Corbett, O. Eboli, J. Gonzalez-Fraile and M. Gonzalez-Garcia, *Constraining anomalous Higgs interactions*, arXiv:1207.1344 [INSPIRE].

[45] P.P. Giardino, K. Kannike, M. Raidal and A. Strumia, *Is the resonance at 125 GeV the Higgs boson?*, arXiv:1207.1347 [INSPIRE].

[46] A. Albaid and K. Babu, *Higgs boson of mass* 125 *GeV in GMSB models with messenger-matter mixing*, arXiv:1207.1014 [INSPIRE].

[47] T. Li, J.A. Maxin, D.V. Nanopoulos and J.W. Walker, *Testing no-scale F*-SU(5): *a* 125 *GeV Higgs boson and SUSY at the* 8 *TeV LHC*, arXiv:1207.1051 [INSPIRE].

[48] R. Benbrik et al., *Confronting the MSSM and the NMSSM with the discovery of a signal in the two photon channel at the LHC*, arXiv:1207.1096 [INSPIRE].

[49] H. Cheon and S.K. Kang, *Constraining parameter space in type-II two-Higgs doublet model in light of a* 125 *GeV Higgs boson*, arXiv:1207.1083 [INSPIRE].

[50] A. Arbey, M. Battaglia, A. Djouadi and F. Mahmoudi, *The Higgs sector of the phenomenological MSSM in the light of the Higgs boson discovery*, arXiv:1207.1348 [INSPIRE].

[51] G. Giudice, C. Grojean, A. Pomarol and R. Rattazzi, *The strongly-interacting light Higgs*, *JHEP* **06** (2007) 045 [hep-ph/0703164] [INSPIRE].

[52] R. Contino, C. Grojean, M. Moretti, F. Piccinini and R. Rattazzi, *Strong double Higgs production at the LHC*, *JHEP* **05** (2010) 089 [arXiv:1002.1011] [INSPIRE].

[53] R. Contino, *The Higgs as a composite Nambu-Goldstone boson*, arXiv:1005.4269 [INSPIRE].

[54] R. Grober and M. Muhlleitner, *Composite Higgs boson pair production at the LHC*, *JHEP* **06** (2011) 020 [arXiv:1012.1562] [INSPIRE].

[55] M. Farina, C. Grojean and E. Salvioni, *(Dys)zphilia or a custodial breaking Higgs at the LHC*, *JHEP* **07** (2012) 012 [arXiv:1205.0011] [INSPIRE].

[56] J. Ellis and T. You, *Global analysis of experimental constraints on a possible Higgs-like particle with mass* ∼ 125 *GeV*, *JHEP* **06** (2012) 140 [arXiv:1204.0464] [INSPIRE].

[57] W.D. Goldberger, B. Grinstein and W. Skiba, *Distinguishing the Higgs boson from the dilaton at the Large Hadron Collider*, *Phys. Rev. Lett.* **100** (2008) 111802 [arXiv:0708.1463] [INSPIRE].

[58] J. Fan, W.D. Goldberger, A. Ross and W. Skiba, *Standard model couplings and collider signatures of a light scalar*, *Phys. Rev.* **D 79** (2009) 035017 [arXiv:0803.2040] [INSPIRE].

[59] L. Vecchi, *Phenomenology of a light scalar: the dilaton*, *Phys. Rev.* **D 82** (2010) 076009 [arXiv:1002.1721] [INSPIRE].

[60] B. Grinstein and P. Uttayarat, *A very light dilaton*, *JHEP* **07** (2011) 038 [arXiv:1105.2370] [INSPIRE].

[61] V. Barger, M. Ishida and W.-Y. Keung, *Dilaton at the LHC*, *Phys. Rev.* **D 85** (2012) 015024 [arXiv:1111.2580] [INSPIRE].

[62] B. Coleppa, T. Gregoire and H.E. Logan, *Dilaton constraints and LHC prospects*, *Phys. Rev.* **D 85** (2012) 055001 [arXiv:1111.3276] [INSPIRE].

[63] B.A. Campbell, J. Ellis and K.A. Olive, *Phenomenology and cosmology of an electroweak pseudo-dilaton and electroweak baryons*, *JHEP* **03** (2012) 026 [arXiv:1111.4495] [INSPIRE].

[64] K. Yamawaki, M. Bando and K.-i. Matumoto, *Scale invariant technicolor model and a technidilaton*, *Phys. Rev. Lett.* **56** (1986) 1335 [INSPIRE].

[65] M. Bando, K.-i. Matumoto and K. Yamawaki, *Technidilaton*, *Phys. Lett.* **B 178** (1986) 308 [INSPIRE].

[66] D.D. Dietrich, F. Sannino and K. Tuominen, *Light composite Higgs from higher representations versus electroweak precision measurements: predictions for CERN LHC*, *Phys. Rev.* **D 72** (2005) 055001 [hep-ph/0505059] [INSPIRE].

[67] K. Yamawaki, *Conformal Higgs, or techni-dilaton-composite Higgs near conformality*, *Int. J. Mod. Phys.* **A 25** (2010) 5128 [arXiv:1008.1834] [INSPIRE].

[68] M. Hashimoto and K. Yamawaki, *Techni-dilaton at conformal edge*, *Phys. Rev.* **D 83** (2011) 015008 [arXiv:1009.5482] [INSPIRE].

[69] T. Appelquist and Y. Bai, *A light dilaton in walking gauge theories*, *Phys. Rev.* **D 82** (2010) 071701 [arXiv:1006.4375] [INSPIRE].

[70] A. Delgado, K. Lane and A. Martin, *A light scalar in low-scale technicolor*, *Phys. Lett.* **B 696** (2011) 482 [arXiv:1011.0745] [INSPIRE].

[71] O. Antipin, M. Mojaza and F. Sannino, *Light dilaton at fixed points and ultra light scale super Yang-Mills*, *Phys. Lett.* **B 712** (2012) 119 [arXiv:1107.2932] [INSPIRE].

[72] S. Matsuzaki and K. Yamawaki, *Techni-dilaton signatures at LHC*, *Prog. Theor. Phys.* **127** (2012) 209 [arXiv:1109.5448] [INSPIRE].

[73] D.B. Kaplan and H. Georgi, $SU(2) \times U(1)$ *breaking by vacuum misalignment*, *Phys. Lett.* **B 136** (1984) 183 [INSPIRE].

[74] D.B. Kaplan, H. Georgi and S. Dimopoulos, *Composite Higgs scalars*, *Phys. Lett.* **B 136** (1984) 187 [INSPIRE].

[75] C. Csáki, J. Hubisz and S.J. Lee, *Radion phenomenology in realistic warped space models*, *Phys. Rev.* **D 76** (2007) 125015 [arXiv:0705.3844] [INSPIRE].

[76] H. de Sandes and R. Rosenfeld, *Radion-Higgs mixing effects on bounds from LHC Higgs searches*, *Phys. Rev.* **D 85** (2012) 053003 [arXiv:1111.2006] [INSPIRE].

[77] K. Cheung and T.-C. Yuan, *Could the excess seen at* 124–126 *GeV be due to the Randall-Sundrum radion?*, *Phys. Rev. Lett.* **108** (2012) 141602 [arXiv:1112.4146] [INSPIRE].

[78] E. Gabrielli, B. Mele and M. Raidal, *Has a fermiophobic Higgs boson been detected at the LHC?*, *Phys. Lett.* **B 716** (2012) 322 [arXiv:1202.1796] [INSPIRE].

[79] G. Cacciapaglia, C. Csáki, G. Marandella and J. Terning, *The gaugephobic Higgs*, *JHEP* **02** (2007) 036 [hep-ph/0611358] [INSPIRE].

[80] S. Weinberg, *Nonlinear realizations of chiral symmetry*, *Phys. Rev.* **166** (1968) 1568 [INSPIRE].

[81] S.R. Coleman, J. Wess and B. Zumino, *Structure of phenomenological lagrangians. 1*, *Phys. Rev.* **177** (1969) 2239 [INSPIRE].

[82] C.G. Callan Jr., S.R. Coleman, J. Wess and B. Zumino, *Structure of phenomenological lagrangians. 2*, *Phys. Rev.* **177** (1969) 2247 [INSPIRE].

[83] A. Salam and J. Strathdee, *Nonlinear realizations. 2. Conformal symmetry*, *Phys. Rev.* **184** (1969) 1760 [INSPIRE].

[84] J.R. Ellis, *Aspects of conformal symmetry and chirality*, *Nucl. Phys.* **B 22** (1970) 478 [inSPIRE].

[85] T. Appelquist and C.W. Bernard, *Strongly interacting Higgs bosons*, *Phys. Rev.* **D 22** (1980) 200 [inSPIRE].

[86] J.R. Ellis, M.K. Gaillard and D.V. Nanopoulos, *A phenomenological profile of the Higgs boson*, *Nucl. Phys.* **B 106** (1976) 292 [inSPIRE].

[87] R. Crewther, *Nonperturbative evaluation of the anomalies in low-energy theorems*, *Phys. Rev. Lett.* **28** (1972) 1421 [inSPIRE].

[88] M.S. Chanowitz and J.R. Ellis, *Canonical anomalies and broken scale invariance*, *Phys. Lett.* **B 40** (1972) 397 [inSPIRE].

[89] M.S. Chanowitz and J.R. Ellis, *Canonical trace anomalies*, *Phys. Rev.* **D 7** (1973) 2490 [inSPIRE].

[90] K. Agashe, R. Contino and A. Pomarol, *The minimal composite Higgs model*, *Nucl. Phys.* **B 719** (2005) 165 [hep-ph/0412089] [inSPIRE].

[91] K. Agashe and R. Contino, *The minimal composite Higgs model and electroweak precision tests*, *Nucl. Phys.* **B 742** (2006) 59 [hep-ph/0510164] [inSPIRE].

[92] R. Barbieri, B. Bellazzini, V.S. Rychkov and A. Varagnolo, *The Higgs boson from an extended symmetry*, *Phys. Rev.* **D 76** (2007) 115008 [arXiv:0706.0432] [inSPIRE].

[93] C. Anastasiou, E. Furlan and J. Santiago, *Realistic composite Higgs models*, *Phys. Rev.* **D 79** (2009) 075003 [arXiv:0901.2117] [inSPIRE].

[94] O. Matsedonskyi, G. Panico and A. Wulzer, *Light top partners for a light composite Higgs*, arXiv:1204.6333 [inSPIRE].

[95] A. Pomarol and F. Riva, *The composite Higgs and light resonance connection*, *JHEP* **08** (2012) 135 [arXiv:1205.6434] [inSPIRE].

[96] D. Marzocca, M. Serone and J. Shu, *General composite Higgs models*, *JHEP* **08** (2012) 013 [arXiv:1205.0770] [inSPIRE].

[97] M. Redi, A. Tesi and A. Tesi, *Implications of a light Higgs in composite models*, arXiv:1205.0232 [inSPIRE].

[98] A. Azatov, R. Contino and J. Galloway, *Model-independent bounds on a light Higgs*, *JHEP* **04** (2012) 127 [arXiv:1202.3415] [inSPIRE].

[99] S. Kraml et al., *Searches for new physics: Les Houches recommendations for the presentation of LHC results*, *Eur. Phys. J.* **C 72** (2012) 1976 [arXiv:1203.2489] [inSPIRE].

[100] S. Matsuzaki and K. Yamawaki, *Techni-dilaton at 125 GeV*, *Phys. Rev.* **D 85** (2012) 095020 [arXiv:1201.4722] [inSPIRE].

[101] S. Matsuzaki and K. Yamawaki, *Discovering 125 GeV techni-dilaton at LHC*, *Phys. Rev.* **D 86** (2012) 035025 [arXiv:1206.6703] [inSPIRE].

[102] D. Carmi, A. Falkowski, E. Kuflik and T. Volansky, *Interpreting LHC Higgs results from natural new physics perspective*, *JHEP* **07** (2012) 136 [arXiv:1202.3144] [inSPIRE].

[103] M. Dührssen et al., *Extracting Higgs boson couplings from CERN LHC data*, *Phys. Rev.* **D 70** (2004) 113009 [hep-ph/0406323] [inSPIRE].

[104] R. Lafaye, T. Plehn, M. Rauch, D. Zerwas and M. Dührssen, *Measuring the Higgs sector*, *JHEP* **08** (2009) 009 [arXiv:0904.3866] [INSPIRE].

[105] M. Klute, R. Lafaye, T. Plehn, M. Rauch and D. Zerwas, *Measuring Higgs couplings from LHC data*, arXiv:1205.2699 [INSPIRE].

[106] A. Azatov et al., *Determining Higgs couplings with a model-independent analysis of* $h \to \gamma\gamma$, *JHEP* **06** (2012) 134 [arXiv:1204.4817] [INSPIRE].